Developmental Cell, Vol. 7, 331–345, September, 2004, Copyright ©2004 by Cell Press

Foxh1 Is Essential for Development of the Anterior Heart Field

Ingo von Both,[1] Cristoforo Silvestri,[2,7] Tuba Erdemir,[1,7] Heiko Lickert,[1] Johnathon R. Walls,[3] R. Mark Henkelman,[3] Janet Rossant,[1,4] Richard P. Harvey,[6] Liliana Attisano,[5] and Jeffrey L. Wrana[1,4,*]

[1]Samuel Lunenfeld Research Institute
Mount Sinai Hospital
600 University Avenue
Toronto, Ontario M5G 1X5
Canada

[2]Institute of Medical Science
University of Toronto

[3]Department of Medical Biophysics

[4]Department of Medical Genetics and Microbiology

[5]Department of Biochemistry
Medical Sciences Building
1 King's College Circle
University of Toronto
Toronto, Ontario M5S 1A8
Canada

[6]Victor Chang Cardiac Research Institute
Faculties of Life Science and Medicine
University of New South Wales
384 Victoria Street
Kensington 2051, New South Wales
Australia

Summary

The anterior heart field (AHF) mediates formation of the outflow tract (OFT) and right ventricle (RV) during looping morphogenesis of the heart. Foxh1 is a forkhead DNA binding transcription factor in the TGFβ-Smad pathway. Here we demonstrate that *Foxh1*$^{-/-}$ mutant mouse embryos form a primitive heart tube, but fail to form OFT and RV and display loss of outer curvature markers of the future working myocardium, similar to the phenotype of *Mef2c*$^{-/-}$ mutant hearts. Further, we show that *Mef2c* is a direct target of Foxh1, which physically and functionally interacts with Nkx2-5 to mediate strong Smad-dependent activation of a TGFβ response element in the *Mef2c* gene. This element directs transgene expression to the presumptive AHF, as well as the RV and OFT, a pattern that closely parallels endogenous *Mef2c* expression in the heart. Thus, Foxh1 and Nkx2-5 functionally interact and are essential for development of the AHF and its derivatives, the RV and OFT, in response to TGFβ-like signals.

Introduction

The heart arises shortly after gastrulation, and problems in heart morphogenesis lead to congenital heart disease, which is the most common form of birth defect in humans (Harvey, 2002a; Olson and Schneider, 2003). Initiation of heart development occurs in the cardiac crescent, or primary heart field, when cells adopt a cardiac fate in response to extracellular cues such as Bone Morphogenetic Proteins (BMPs), Fibroblast Growth Factors (FGFs), and Wingless related factors (WNTs). Cells from this primary heart field then contribute to the developing linear heart tube, which in mammals is composed largely of prospective left ventricle (LV) (Cai et al., 2003). At the looping stage, there is a large expansion at the arterial pole of the developing heart in the RV and OFT region that occurs concomitantly with rightward looping of the linear heart tube (Kelly and Buckingham, 2002). At this early stage, regional specification of the heart chambers is already evident. For example, *Hand2* (formerly *dHand*) and *Mef2c*, which encode bHLH and MADS box transcription factors, respectively, display restricted expression to the RV and OFT, and deletion of these genes leads to defects in RV and OFT morphogenesis (Lin et al., 1997; Srivastava et al., 1997).

Early analysis of heart development in the mouse and fate mapping studies in the chick suggest that the OFT does not arise from the primary heart field but is added later from a distinct population of cells (Kelly et al., 2001; Kelly and Buckingham, 2002; Mjaatvedt et al., 2001; Waldo et al., 2001). This secondary, or anterior, heart-forming field (AHF) arises from a group of splanchnic mesodermal cells that lie medial to the primary heart field cells and extend anterior and dorsal to the early linear heart tube. Furthermore, in the mouse, fate mapping together with analysis of the *Fgf10* gene suggests that as the arterial pole of the heart undergoes rapid expansion, a group of *Fgf10*-expressing cells in the pharyngeal mesoderm contribute to splanchnic mesoderm and thence to the growing heart tube (Kelly et al., 2001). The AHF is thus thought to be a critical precursor population for formation of the RV and OFT.

Little is known of the signals that regulate formation of the AHF. However, BMPs are expressed in the AHF (Waldo et al., 2001) and likely function to induce expression of the pancardiac homeobox gene *Nkx2-5*, which is essential for myocardial differentiation in vitro and cardiac morphogenesis and chamber differentiation in vivo (Cripps and Olson, 2002; Harvey, 2002b; Olson and Schneider, 2003). Expression of *Fgf8* and *Fgf10* also marks the AHF and may regulate cardiomyocyte differentiation or the migratory behavior of precursor cells destined to move into the arterial pole (Kelly and Buckingham, 2002). The medial splanchnic mesoderm that contributes to the AHF also expresses the LIM homeodomain protein Isl1, and in mouse embryos lacking *Isl1,* expression of local BMP and FGF genes is downregulated (Cai et al., 2003). Although Isl1-positive cells may contribute cardiomyocytes to both the anterior and posterior poles of the heart, the most pronounced defects in the mutants are in anterior regions (Cai et al., 2003). This suggests that *Isl1* is important for expression of morphogens that control cardiac development and the specification of splanchnic mesoderm that gives rise

*Correspondence: wrana@mshri.on.ca
[7]These authors contributed equally to this work.

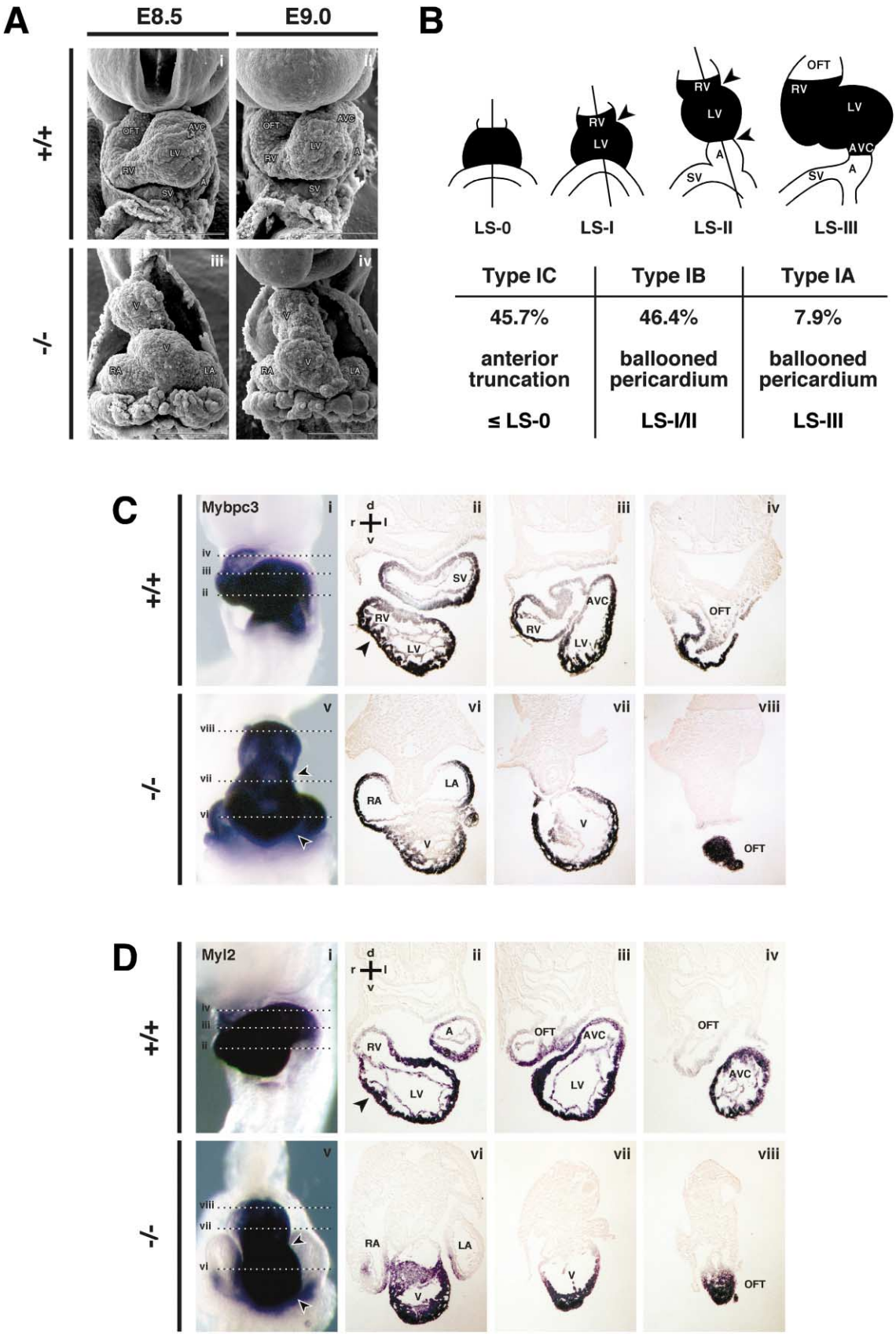

Figure 1. Defects in Heart Morphology in *Foxh1*$^{-/-}$ Mutant Embryos

(A) Scanning electron microscopy analysis of stage matched wild-type (+/+) and *Foxh1* null mutant (−/−) embryos at embryonic days E8.5 and E9.0. Frontal views of each embryo are shown with the pericardium removed. Most *Foxh1*$^{-/-}$ mutant embryo hearts (iii, iv) arrest by LS-II with disorganized primitive ventricles. Scale bar 200 μm.

to the AHF. Of note, the forkhead DNA binding protein Foxh1, previously named FAST2 (Labbe et al., 1998), is strongly expressed in the heart-forming regions during the looping stage (Weisberg et al., 1998). Since Foxh1 is a nuclear target of the Transforming Growth Factor β (TGFβ)-Smad signaling pathway (Attisano et al., 2001), this suggests that TGFβ-like signals may also function to regulate heart morphogenesis.

TGFβ signals through heteromeric complexes of transmembrane Ser/Thr kinase receptors that phosphorylate receptor-regulated (R)-Smad2 and R-Smad3. This induces assembly of a R-Smad-Smad4 complex and nuclear accumulation of the heteromeric Smad complex. In the nucleus, R-Smad2 and R-Smad3 interact with DNA binding proteins, such as Foxh1, while Smad4 stabilizes DNA binding by the ternary complex and recruits coactivators. Since Foxh1 only binds R-Smad2 and R-Smad3, it functions specifically to transduce TGFβ-like signals into transcriptional responses (Labbe et al., 1998). Genetic analyses in zebrafish and mouse have shown a key role for Foxh1 in mediating anterior-posterior patterning by nodal-like signals during gastrulation (Whitman, 2001). In zebrafish, Foxh1 is the product of the *schmalspur* gene and mutations in the region of this gene encoding the forkhead DNA binding domain lead to loss of the gastrula organizer and subsequent loss of axial midline structures (Whitman, 2001). In the mouse, deletion of *Foxh1* leads to constrictions at the embryonic-extraembryonic boundary with lack of anterior specification, primitive streak elongation, and subsequent failure of gastrulation (Type II and III mutants) (Hoodless et al., 2001; Yamamoto et al., 2001). This occurs with variable penetrance, and in less severe Type I mutants, defects in specification of the anterior primitive streak that are analogous to the zebrafish *schmalspur* mutants are observed, with subsequent loss of midline structures (Hoodless et al., 2001; Yamamoto et al., 2001).

The molecular mechanisms that control formation of the AHF in the mouse are unknown. Here we demonstrate that *Foxh1* is required for formation of the AHF. Accordingly, *Foxh1*$^{-/-}$ mutant embryos exhibit loss of Fgf8- and Fgf10-positive AHF cells and severe defects in RV and OFT formation that closely resemble the defects seen in *Mef2c*$^{-/-}$ mutant hearts. Indeed, we demonstrate that *Mef2c* expression in the anterior region of the heart is dependent on Foxh1 and identify a composite Foxh1-Nkx2-5 binding site within the *Mef2c* gene that is regulated by TGFβ signaling in a Smad-dependent manner. Furthermore, analysis of a *lacZ*-transgene driven by an intronic enhancer fragment of *Mef2c* harboring this element shows Foxh1-dependent expression in the presumptive AHF and its derivatives, the RV and OFT, where endogenous *Mef2c* is expressed. These results thus demonstrate that a TGFβ-like Smad signaling pathway specifies the AHF through a Foxh1-Nkx2-5 complex that regulates *Mef2c* expression.

Results

Heart Defects in *Foxh1* Null Embryos

Foxh1 is expressed throughout the gastrulating embryo, including the region corresponding to the AHF, and at later stages of development it becomes increasingly restricted to the heart (Supplemental Figure S1 [http://www.developmentalcell.com/cgi/content/full/7/3/331/DC1] and Weisberg et al., 1998). In the course of analyzing *Foxh1*$^{-/-}$ mutant embryos (Hoodless et al., 2001), we observed pericardial edema (data not shown), suggesting a defect in heart morphogenesis. Therefore, we investigated the gross morphology of *Foxh1*$^{-/-}$ mutant hearts by scanning electron microscopy. The inflow region of the mutant hearts, including the developing left and right atrial appendages, appeared similar to that of wild-type embryos (Figure 1A). However, the ventricle and OFT of the *Foxh1*$^{-/-}$ mutant hearts were disorganized, particularly at later developmental stages around E9.0. Analysis of looping stage (LS) development in Type I *Foxh1*$^{-/-}$ mutants (Hoodless et al., 2001) showed that hearts in 46% of mutants developed to LS-I/II, 8% developed to LS-III with looping always occurring to the right, and the remaining 46% arrested at LS-0 (Figure 1B). Next, we analyzed expression of the gene encoding cardiac myosin binding protein C *(Mybpc3)*, which is a general cardiomyocyte marker (Bruneau et al., 2001). Comparison to wild-type embryos revealed that overall expression in mutant embryos was not grossly abnormal, indicating no major defect in cardiomyocyte differentiation (Figure 1C). However, serial sections revealed a disorganized myocardium, poor trabeculation in the ventricular region, and a very poorly formed OFT (Figure 1C, vi–viii). Further, posterior development appeared normal, as clearly defined right and left atria were evident in the mutants (Figure 1C, vi). Analysis of expression of the pan-cardiomyocyte marker, α cardiac actin *(Actc1)*, showed similar results (data not shown). To further explore the morphology of the mutant hearts, we employed optical projection tomography (OPT), which allows for three-dimensional imaging of fluorescently stained embryos (Sharpe et al., 2002). In striking contrast to wild-type embryos, *Foxh1* mutants costained for Mybpc3 and Actc to highlight all of the cardiomyocytes displayed a poorly formed OFT that ended in a blind sac (Supplemental Movie S1). Next, we analyzed myosin light chain 2v (*Myl2*), an early marker of the ventricular region (Christoffels et al., 2000). *Myl2* showed robust expression in the future ventricle region of the abnormal mutant hearts (Figure 1D), indicating that they had attained ventricular identity. However, as also highlighted

(B) Schematic (top) of early stages of cardiac looping morphogenesis in mouse embryos and summary (bottom) of the gross morphology and observed LS of hearts in Type I *Foxh1*$^{-/-}$ mutants (percent of 140 Type I *Foxh1*$^{-/-}$ mutants analyzed) (Hoodless et al., 2001; Yamamoto et al., 2001).

(C and D) Whole-mount in situ staining for the pancardiomyocyte marker, *Mybpc3* (C) or the panventricle marker, *Myl2* (D) in E8.5–E8.75 wild-type (+/+, i–iv) and *Foxh1*$^{-/-}$ mutant (−/−, v–viii) embryos. Corresponding sections from each embryo are shown progressively from posterior (ii and vi) to anterior (iv and viii), as indicated in the whole-mount panel (i and v). The black arrowhead marks the left/right ventricular boundary in the sections of the wild-type embryos (ii) and the white/black arrowhead the putative left ventricular segment in the mutant embryos (v).

Abbreviations: LS, looping stage; SV, sinus venosus; A, atria; RA, right atrium; LA, left atrium; AVC, atrioventricular canal; LV, left ventricle; RV, right ventricle; V, ventricle; OFT, outflow tract; r, right; l, left; a, anterior, p, posterior; d, dorsal; v, ventral.

by *Mybpc3* expression, the ventricles of the mutants were disorganized and there was an absence of well-formed aortic arch arteries in the region of the aortic sac (Figures 1C and 1D, viii). We also examined *Hey2*, which is also expressed in the ventricle region, and observed expression throughout the heart tube (data not shown). Type IC mutants, which arrest at LS-0 and display severe anterior truncations, revealed similar expression of these markers (data not shown). Thus, *Foxh1*$^{-/-}$ mutants have a common ventricle and form a rudimentary heart tube.

RV and OFT Defects in *Foxh1*$^{-/-}$ Mutants

To understand the molecular basis for the *Foxh1*$^{-/-}$ mutant heart phenotype, we examined markers of chamber specification. *GATA binding protein 4 and 6 (Gata4, Gata6)*, which are expressed in endoderm and cardiomyocytes in the posterior aspect of the heart (Parmacek and Leiden, 1999), were strongly expressed in the mutants (Figure 2A), as was *Myh6* (cardiac myosin heavy chain α), which is normally expressed in the inflow tract and atria at this stage (Figure 2A). Next, we examined the predominantly LV marker *Hand1* (formerly *eHand*) (Brand, 2003; Olson and Schneider, 2003), which displayed robust expression in the prospective LV of the mutants (Figure 2B). In striking contrast, expression of *Smpx* (Chisel) and *Nppa* (Atrial Natriuretic Factor), which are normally expressed in the outer curvature of the left and right ventricles, as well as the forming atrial appendages (Christoffels et al., 2000), were completely absent in the ventricular region of mutant hearts, although still present in the future atrial region (Figure 2C). *Nppa* expression is regulated by Tbx5 (Bruneau et al., 2001). Therefore, we examined *Tbx5* expression, which was found to be normal in the inflow tract of *Foxh1*$^{-/-}$ mutant hearts, but was undetectable in the LV (Figure 2C). Finally, we examined expression of *Hand2*, which after looping becomes restricted to the RV-OFT (Thomas et al., 1998) and regulates *Nppa* directly (Thattaliyath et al., 2002), as well as *Wnt11*, which marks the OFT (Cai et al., 2003). Neither *Hand2* nor *Wnt11* was expressed at significant levels in stage-matched mutants (Figure 2D). Together, these data indicate that while posterior markers of heart patterning are not severely affected by loss of Foxh1, markers of the RV-OFT are absent and there are defects in patterning the outer curvature of the LV. Of note, the RV-OFT defects coupled with the loss of *Nppa* and *Hand2* expression are highly reminiscent of the null phenotype of *Mef2c* (Lin et al., 1997).

Mutation of *Foxh1* causes defects in specifying the anterior primitive streak during gastrulation, which leads to defects in anterior mesendoderm formation (Hoodless et al., 2001). Similar defects also occur in embryonic mutants of the forkhead protein, *Foxa2* (Dufort et al., 1998), and indeed *Foxa2* expression in the anterior primitive streak is dependent on *Foxh1* (Hoodless et al., 2001). Therefore, to explore whether the patterning defects in *Foxh1* mutant hearts might be caused by a failure in mesendoderm structures, we examined patterning in *Foxa2* embryonic mutant hearts. Although the anterior morphology of *Foxa2* embryonic mutant embryos was disturbed, expression of *Smpx*, *Nppa*, and *Wnt11* was detected in the heart at intensities comparable to wild-type embryos (Supplemental Figure S2A–S2C), contrasting *Foxh1* mutants (Figures 2C and 2D). Moreover, in chimeric embryos comprised of high contributions of *Foxh1* mutant ES cells in a wild-type background, hearts displayed a rudimentary phenotype, despite the strong contribution of wild-type cells to the endoderm (Hoodless et al., 2001). Finally, we examined ES cells that were induced to form beating foci of cardiomyocytes after differentiation into embryoid bodies (EBs) (Supplemental Figure S2D) (Boheler et al., 2002). As shown in Supplemental Figure S2E, EBs comprised of *Foxh1*$^{-/-}$ ES cells (FKO3) were completely defective in their ability to form beating foci, and re-expression of a *Foxh1* transgene restored this capability in a dose-dependent manner. In contrast, *Foxa2*$^{-/-}$ ES lines formed beating foci at a frequency comparable to wild-type ES cells. Altogether, these data indicate that the patterning defects observed in *Foxh1* mutant hearts are not secondary to loss of anterior mesendoderm structures, particularly defects in definitive endoderm.

Defective Anterior Heart Field in *Foxh1*$^{-/-}$ Mutants

The AHF is a key contributor of cardiogenic precursor cells to the RV-OFT of mammalian hearts (Kelly and Buckingham, 2002). *Fgf8* and *Fgf10* gene transcripts mark the AHF and are also expressed in the pharyngeal mesoderm that is contiguous with this structure in anterior regions (Kelly et al., 2001). Therefore, to explore whether the *Foxh1*$^{-/-}$ mutant phenotype reflects defects in the AHF, we examined *Fgf8* and *Fgf10* expression in *Foxh1*$^{-/-}$ mutant embryos. At E8.0, *Fgf8* and *Fgf10* expression appears to mark a distinct population of splanchnic mesodermal cells that lies medial to the primary heart field and which progressively comes to occupy a position dorsal and anterior to the primary heart field, from where it converges at the midline and enters the arterial pole of the developing heart. In mutants at this stage, posterior expression of both *Fgf8* and *Fgf10* was normal; however, there was a marked reduction in expression in the anterior region (Figure 3A), which was most evident at E8.25 when anterior expression of *Fgf8* was absent in the mutants, despite normal posterior expression. Furthermore, at later stages *Foxh1*$^{-/-}$ mutants showed little detectable expression of *Fgf8* and *Fgf10* in the heart field, whereas expression of these markers in the surrounding pharyngeal mesoderm was readily detectable (Figure 3A). Next we examined *Isl1*, which is required for development of the medial splanchnic mesoderm from which FGF-expressing AHF cells arise. Consistent with an early role in specifying the secondary heart field, *Isl1*-expressing cells have been found to contribute to both posterior and anterior segments of the developing heart, and in *Isl1* mutants BMP expression is downregulated in addition to FGFs. In *Foxh1* mutants, *Isl1* expression was similar to wild-type embryos at both E8.0 and E8.5 (Figure 3B) and BMP2 and BMP7 expression was unaffected (data not shown). Together, these results suggest that Foxh1 is not required for development of the Isl1-positive medial splanchnic mesoderm per se, but is required for formation of the AHF, which arises from this population of cells.

Mef2c Expression Is Dependent on Foxh1

Chamber specification in the vertebrate heart is controlled by a hierarchical transcription factor network that

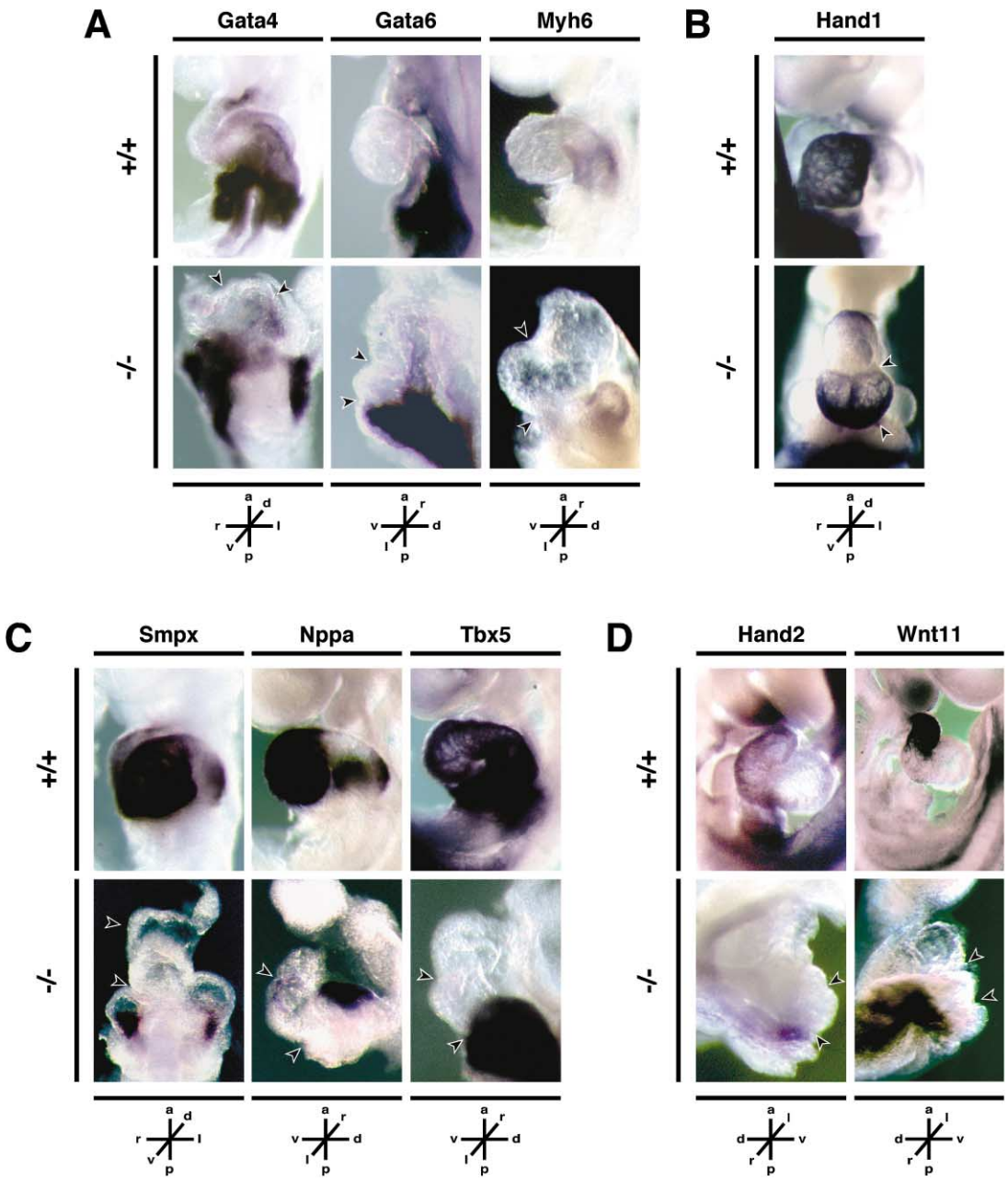

Figure 2. Chamber Specification in *Foxh1*$^{-/-}$ Mutant Embryos

Embryos between E8.5 and E9.0 were hybridized with the indicated digoxigenin-labeled riboprobes. Only the heart region, with pericardium removed, is shown for each stage-matched embryo. The anterior and posterior boundaries of the prospective left ventricle in the *Foxh1*$^{-/-}$ mutant hearts are marked (arrowheads).

(A) The inflow tract markers *Gata4*, *Gata6*, and *Myh6* are expressed in *Foxh1*$^{-/-}$ mutant hearts.

(B) *Hand1*, which marks the prospective LV region is expressed in the ventricular region of *Foxh1*$^{-/-}$ mutant hearts.

(C) *Smpx* and *Nppa*, which mark the outer curvature of the developing ventricles and *Tbx5* in the LV, are severely downregulated in *Foxh1*$^{-/-}$ mutant hearts. Note that *Nppa*, *Smpx*, and *Tbx5* expression domains in the inflow tract are undisturbed in the *Foxh1*$^{-/-}$ mutants.

(D) *Hand2* and *Wnt11*, which mark the OFT-RV and OFT, respectively, are not expressed in *Foxh1*$^{-/-}$ mutant hearts at E9.0.

includes Nkx2-5 and Mef2c (Brand, 2003; Cripps and Olson, 2002). *Nkx2-5*, which is important for myocardial differentiation in vitro and heart morphogenesis in vivo (Olson and Schneider, 2003), is also required for deployment of AHF cells, and its expression there involves distinct regulatory elements (Schwartz and Olson, 1999). Furthermore, a null mutation in *Mef2c*, which has been proposed to reflect defects in AHF formation (Kelly and Buckingham, 2002), causes RV-OFT defects that are similar to the *Foxh1*$^{-/-}$ heart phenotype. In particular, hearts of both mutants fail to express *Nppa* in their prospective ventricular regions and *Hand2* in the RV-OFT (Lin et al., 1997) (Figures 2C and 2D). This prompted us to examine *Nkx2-5* and *Mef2c*, which are at the top of this hierarchical transcription factor network. Strikingly, while *Nkx2-5* expression in the mutants was normal,

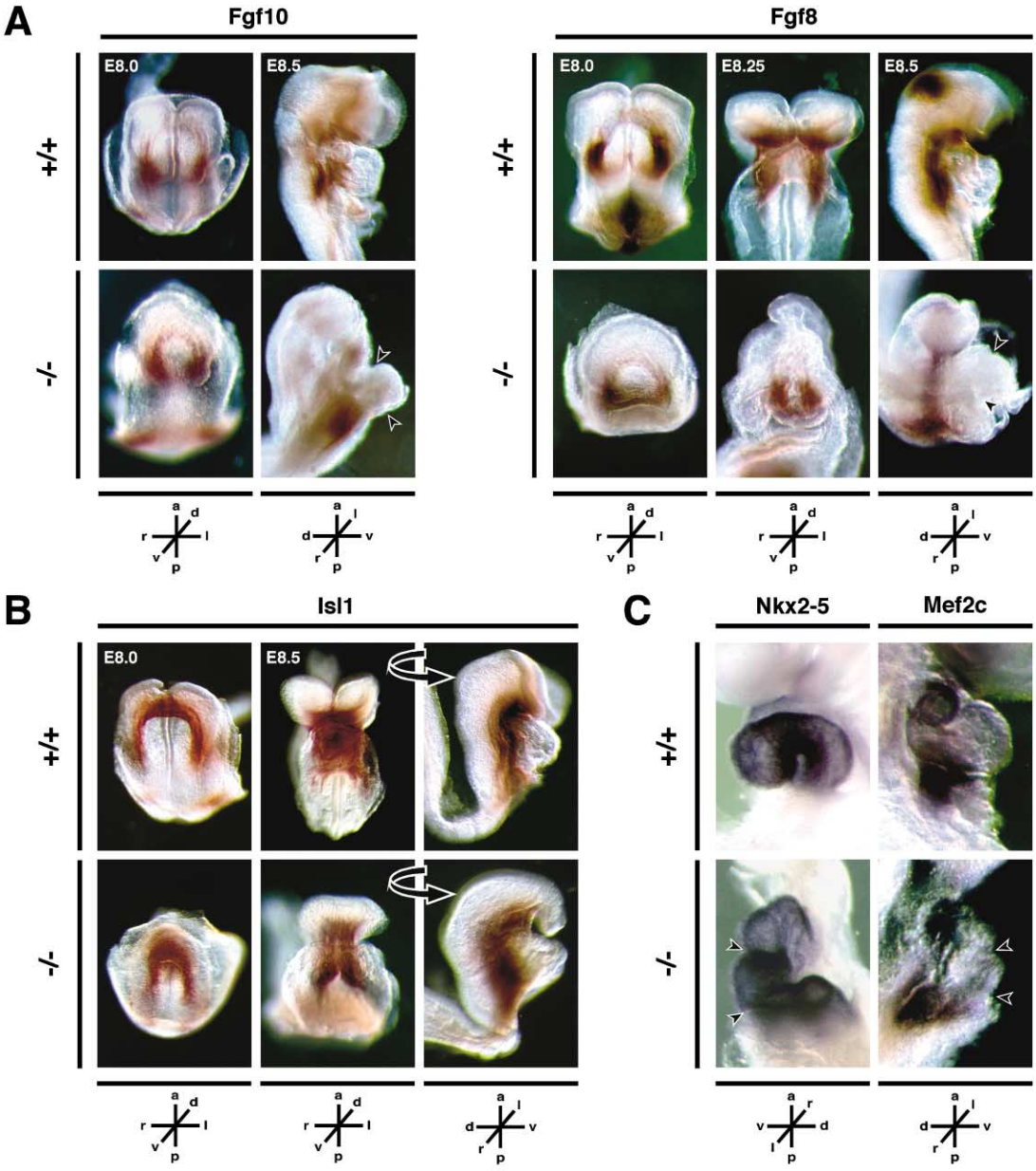
A
Fgf10
Fgf8
E8.0
E8.5
E8.25
+/+
-/-
B
Isl1
C
Nkx2-5
Mef2c
D
Mef2c
Mef2b
Relative mRNA Levels
1.2
1
.8
.6
.4
.2
0
3
2.5
2
1.5
.5
+/+
+/-
-/-

Mef2c expression in the ventricles and OFT was absent, although inflow tract expression of *Mef2c* was still evident (Figure 3C). To confirm this, we performed quantitative real-time RT-PCR on RNA extracted from E8.5 embryos using primers for the cardiac-specific transcript of *Mef2c*. In RNA isolated from *Foxh1*$^{+/-}$ embryos, *Mef2c* expression was decreased to 50% of wild-type, whereas in *Foxh1*$^{-/-}$ mutants the levels were less than 20% of the controls (Figure 3D). We also examined *Mef2b* expression, which is upregulated in *Mef2c*$^{-/-}$ mutants (Lin et al., 1997), and found that it was increased by 2.5-fold in *Foxh1*$^{-/-}$ mutants (Figure 3D). These data show that Foxh1 is critical for development of the AHF and formation of the RV-OFT in part by regulating expression of *Mef2c*, a key component of the cardiac transcription factor gene network.

Foxh1 Interacts with Nkx2-5 to Regulate a TGFβ-Responsive Element in the *Mef2c* Gene

To determine whether Foxh1 might directly regulate *Mef2c*, we searched for Foxh1 binding sites in the *Mef2c* gene and found five candidates, two of which are found close to each other within Fi3A (Figure 4A). We cloned each of these regions into a heterologous luciferase reporter plasmid carrying the E1b basal promoter and tested them for TGFβ- and Foxh1-responsiveness using HepG2 cells, which do not express Foxh1 (Labbe et al., 1998). Of the four elements tested, only Fi3A was found to be TGFβ-responsive in a Foxh1-dependent manner (Figure 4B), although the overall activity was low. *Mef2c* expression is also dependent on Nkx2-5 (Cripps and Olson, 2002), so we also tested these elements in the presence of Nkx2-5 expression. Nkx2-5 induced Fi3A activity but did not allow for TGFβ-responsiveness on its own. However, when Nkx2-5 was coexpressed with Foxh1, the two synergistically activated Fi3A and increased TGFβ-dependent activation of the element to 80-fold over the control. Of note, Fi9 also showed Nkx2-5 responsiveness but it neither synergized with Foxh1 nor displayed TGFβ-dependent regulation, whereas the other two elements displayed no response to any treatment (Figure 4B). The Fi3A construct was therefore chosen for further examination.

Foxh1 interacts with R-Smad2-Smad4 complexes that are in the TGFβ pathway, to form a Foxh1-Smad complex on DNA (Labbe et al., 1998). Therefore, we overexpressed R-Smad2 and Smad4 in HepG2 cells and evaluated Fi3A activation. R-Smad2 and Smad4 had minimal effects when expressed with Foxh1 alone, but when Nkx2-5 was coexpressed, the Smads significantly increased activation of the enhancer (Figure 4C). Furthermore, expression of a Foxh1 mutant (Foxh1-SIMm), which is defective in Smad binding (Germain et al., 2000), abolished all TGFβ responsiveness, as did a Foxh1 mutant (Foxh1-FKHDm) that is defective in its forkhead DNA binding domain (Figure 4C). We also observed that Fi3A was unresponsive to BMP2 stimulation (Figure 4C), consistent with the specific function of Foxh1 in TGFβ-like signaling pathways (Labbe et al., 1998). Therefore, TGFβ-dependent activation of Fi3A is dependent on both the Smad binding and forkhead DNA binding activity of Foxh1.

The Fi3A element contains two potential Foxh1 binding sites (Figure 4D). Mutation of the upstream site (Fi3A-F1m) had no effect on Fi3A activation, whereas mutation of the downstream site (Fi3A-F2m) abolished all TGFβ-responsiveness (Figure 4E). We noted that this Foxh1 site is situated two base pairs upstream of an Nkx2-5 consensus binding site and has adjacent Smad binding elements (Figure 4D), suggesting that Foxh1 and Nkx2-5 synergize through this element. To test this, we generated a 132 bp element that incorporated the Foxh1, Nkx2-5, and Smad binding elements (FNE, for Foxh1 and Nkx2-5 element; Figure 4D). Analysis of the wild-type FNE revealed that it responded to TGFβ in a Foxh1- and Nkx2-5-dependent manner (Figure 4F), whereas mutation of the Foxh1 and Nkx2-5 sites (FmNE and FNmE, respectively; Figure 4D) abolished responsiveness (Figure 4F). Thus, activation of the TGFβ-responsive FNE within intron 3 of *Mef2c* is dependent upon adjacent Foxh1 and Nkx2-5 binding sites.

To characterize binding of Foxh1 and Nkx2-5 to the FNE, we employed a DNA immunoprecipitation approach using COS1 cells expressing Nkx2-5 or Foxh1 (see Experimental Procedures). In either Foxh1 or Nkx2-5 immunoprecipitates, we readily detected the bound FNE (Figure 5A), and mutation of the Foxh1 forkhead domain abolished Foxh1 binding (data not shown). We also confirmed by electrophoretic mobility shift assays that Foxh1 and Nkx2-5 bound to FNE (data not shown). To demonstrate that Foxh1 occupies the endogenous *Mef2c* FNE during cardiomyocyte differentiation, we employed

Figure 3. *Foxh1* Is Required for the Anterior Heart Field and *Mef2c* Expression

(A) Defects in the anterior heart field of *Foxh1*$^{-/-}$ mutants. Wild-type (+/+) and *Foxh1* null mutant (−/−) embryos at E8.0 and E8.25–E8.5 (indicated) were analyzed by whole-mount in situ for *Fgf10* (left panels) and *Fgf8* (right panels) expression. At the earlier stage, both *Fgf10* and *Fgf8* are expressed in *Foxh1*$^{-/-}$ mutants in the splanchnic mesoderm that lies medial to the cardiac crescent, whereas at later stages anterior expression is decreased relative to controls. This is most prominent in mutant hearts at the linear heart tube stage (E8.25). At the early looping stage, expression in the OFT-RV of mutant hearts is absent, whereas expression in the surrounding mesoderm is evident.

(B) Analysis of *Isl1* expression. Ventral views of E8.0 (left) and E8.5 (middle) wild-type (+/+) and *Foxh1* null mutant (−/−) embryos analyzed for *Isl1* expression with a right lateral view of the E8.5 embryo also shown (right). Note that *Isl1* expression in the mutants is comparable to wild-type patterns.

(C) Analysis of *Nkx2-5* and *Mef2c* expression. Left lateral (Nkx2-5) and right lateral (Mef2c) views of wild-type (+/+) and *Foxh1* null mutant (−/−) embryos analyzed for *Nkx2-5* and *Mef2c* expression by whole-mount in situ. Note that while *Nkx2-5* is expressed throughout mutant hearts, *Mef2c* expression is absent in the poorly formed OFT and RV, but not in the posterior domain. Arrowheads mark anterior and posterior boundaries of the LV in mutant embryos.

(D) Analysis of *Mef2* family member expression. RNA purified from E8.5 wild-type, *Foxh1*$^{+/-}$, and *Foxh1*$^{-/-}$ embryos (+/+, +/−, −/−, respectively) was analyzed by real-time PCR using primers specific for *Mef2b* or the cardiac transcript of *Mef2c*. Results are plotted relative to the wild-type control (mean ± SD) for each gene.

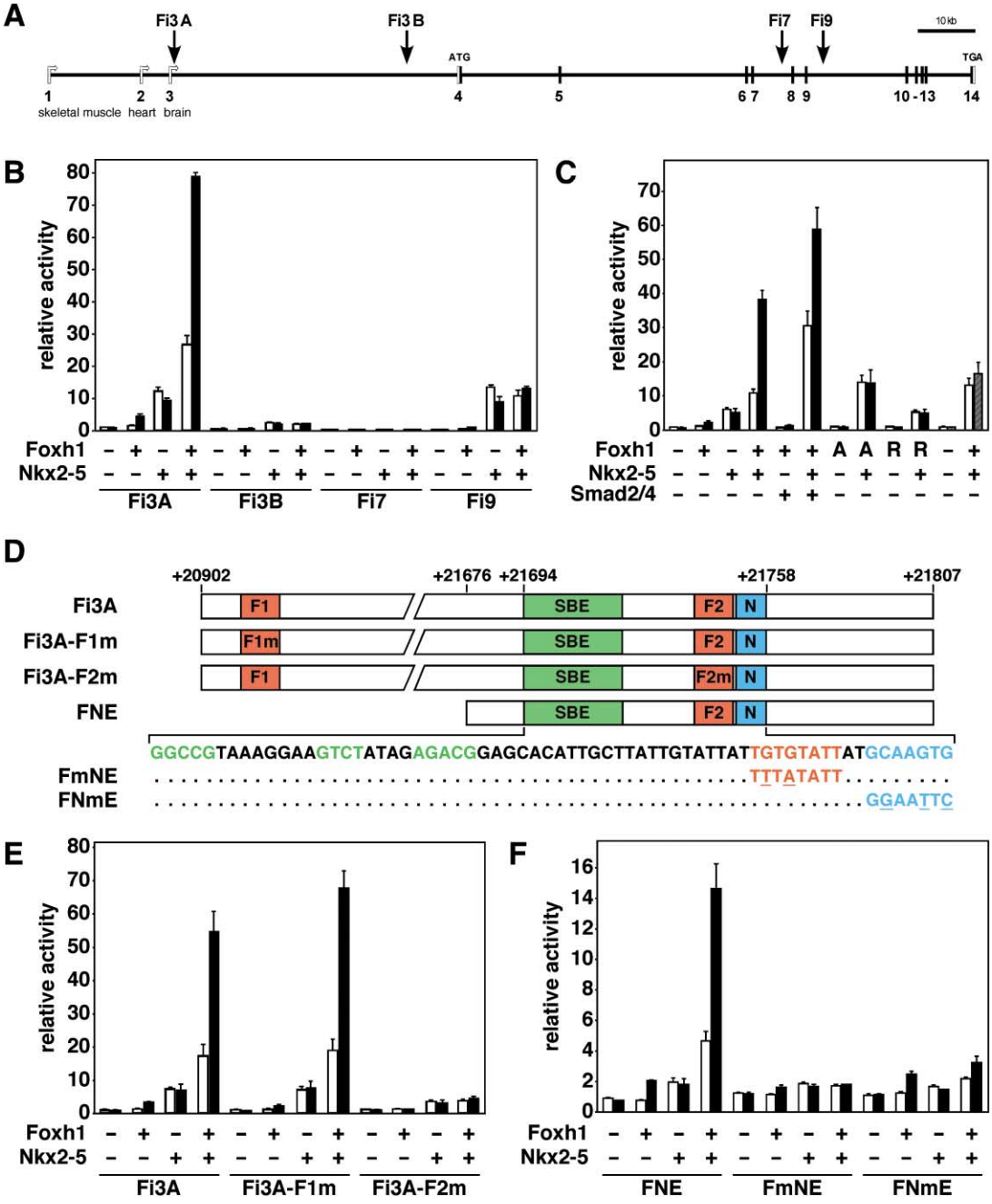

Figure 4. Nkx2-5 and Foxh1 Synergize to Regulate TGFβ Responsiveness of an Intron Enhancer in the *Mef2c* Gene

(A) Schematic representation of the *Mef2c* gene. Numbered boxes depict exons of untranslated and translated regions in white and black, respectively (Wang et al., 2001). Open right angle arrows indicate tissue-specific transcription start sites, and closed arrows show the relative positions of Foxh1 sites in the introns (Fi3A, Fi3B, Fi7, Fi9).

(B, C, E, and F) Luciferase reporter assays. HepG2 cells were transiently transfected with the indicated *Mef2c-Luc* reporter constructs with (+) and without (−) Foxh1, Nkx2-5, Smad2, or Smad4 expression constructs. Luciferase activity in lysates from cells incubated overnight in the absence (white bars) or presence of 100 pM TGFβ (black bars) or 1 nM BMP2 (hatched bars) was determined and normalized to β-galactosidase activity. Data are presented as fold activation over basal promoter activity (relative activity), and are expressed as mean ± SD of triplicates from a representative experiment. (C) Activity of *Mef2c-Fi3A-Luc*. *Mef2c-Fi3A-Luc* activity was assayed in the presence of wild-type Foxh1 (+), the Foxh1 SIMm mutant (A), the Foxh1 FKHDm mutant (R), and the indicated combinations of Nkx2-5, Smad2, and Smad4.

(D) Schematic representation of the 906 bp Fi3A element and its derivatives. Smad (SBE, green), Foxh1 (F1 or F2, red), and Nxk2-5 (N, blue) sites and their corresponding mutants (F2m and Nm) are indicated. Numbering is according to GenBank #NT_039589.

(E) Activity of Fi3A and derivatives containing mutations in either the first (Fi3A-F1m) or second (Fi3A-F2m) Foxh1 sites. (F) Characterization of FNE. A minimal TGFβ-responsive element (FNE, for Foxh1 and Nkx2-5 element) was identified in Fi3A and Foxh1 (FmNE) and Nkx2-5 (FNmE) site mutants tested as indicated.

chromatin immunoprecipitation (ChIP) using ES cells differentiated into cardiomyocytes (Supplemental Figure S2D) (Boheler et al., 2002). For this, we subjected *Foxh1*$^{-/-}$ ES cells reconstituted with Flag-tagged Foxh1 (clone PF13) or the control R1 wild-type ES cell line to in vitro EB differentiation (Supplemental Figure S2E) and performed ChIP. As shown in Figure 5B, the region of the *Mef2c* gene corresponding to the FNE was readily apparent in Foxh1, but not in control nor differentiated R1 ES cell immunoprecipitates. Furthermore, analysis of Flag-Foxh1 immunoprecipitates using primers located 3.2 kb upstream of the FNE yielded no product, confirming specific Foxh1 binding to the sheared FNE fragment (data not shown). To determine if Foxh1 and Nkx2-5 co-occupy the FNE, we next employed a two-step DNA immunoprecipitation procedure (Benchabane and Wrana, 2003). For this, protein-DNA complexes in either Foxh1 or Nkx2-5 immunoprecipitates were isolated, eluted, and then subjected to a second immunoprecipitation using the opposite antibody. In cells expressing either Foxh1 or Nkx2-5 alone, no FNE was detected in the double immunoprecipitate, whereas PCR product was readily detected in cells coexpressing Foxh1 and Nkx2-5 (Figure 5C). Thus, Foxh1 and Nkx2-5 can co-occupy the *Mef2c* FNE.

Co-occupation of the FNE suggested the possibility that Foxh1 and Nkx2-5 physically associate. To investigate this, we tested Foxh1 immunoprecipitates for the presence of Nkx2-5 and observed that Nkx2-5 coprecipitated with Foxh1 (Figure 5D). Bacterially expressed Nkx2-5 also interacted with Foxh1, indicating the interaction is direct. Mutation of the Foxh1 forkhead domain (FKHDm) abrogated this interaction, whereas the Smad binding domain mutants (SIMm and ΔSID) had no effect (Figure 5E). We next examined Nkx2-5 mutants and observed reduced binding upon removal of the first 136 amino acids of Nkx2-5 and undetectable association upon deletion of the homeodomain (ΔNHD and ΔHD). The homeodomain alone was also able to bind Foxh1 to some degree (Figure 5F). Therefore, the amino-terminal-homeodomain region of Nkx2-5 is important for efficient binding to Foxh1. To determine if the physical interaction between Nkx2-5 and Foxh1 is important for activation of the FNE, we focused on Nkx2-5(ΔN) which decreased Foxh1 binding but does not interfere with Nkx2-5 DNA binding activity (data not shown). While the increase in FNE activity induced by expressing Nkx2-5 on its own was unaffected by this deletion, synergism with Foxh1 was significantly decreased (Figure 5G). The residual co-operativity likely reflects retention of some Foxh1 binding activity mediated by the homeodomain. In contrast, deletion of the homeodomain abolished both Nkx2-5-dependent activation of the FNE and synergism with Foxh1, consistent with the notion that the homeodomain of Nkx2-5 is also critical for the interaction, as demonstrated in vitro (Figure 5G). Collectively, these data indicate that Foxh1 and Nkx2-5 physically interact and cooperate to mediate synergistic TGFβ- and Smad-dependent activation of an FNE present in the *Mef2c* gene.

The FNE Directs Transgene Expression in the AHF and RV-OFT

To determine if the FNE is active in vivo, we generated two transgenes in which either wild-type Fi3A or the nonresponsive Foxh1 mutant, Fi3A-F2m, were linked to the hsp68 promoter to drive expression of *lacZ*. After generating stable transfectants in ES cells, we first characterized transgene activity in vitro using ES cells differentiated into EBs (see Supplemental Figure S2D for further details). After plating EBs on gelatin-coated dishes, beating foci were marked and the cells then processed to detect *lacZ* activity. In ES cells harboring the wild-type *Fi3A-hsp68LacZpA* transgene (clone S1-2), 100% of beating foci stained for lacZ with minimal staining observed in nonbeating cells (Figure 6A). We also analyzed a second ES line harboring the wild-type *Fi3A-hsp68LacZpA* transgene (clone S1-6) and observed similar expression in beating foci (data not shown). In contrast, none of the ES cell lines with the *Fi3A-F2m-hsp68LacZpA* mutant transgene displayed detectable *lacZ* expression (Figure 6A and data not shown). Next, we analyzed these lines using tetraploid aggregation, which leads to 100% contribution of ES cells to the embryo (Nagy et al., 2003). Analysis of tetraploids derived from clone S1-2, which harbors the wild-type *Fi3A-hsp68LacZpA* transgene, revealed staining in the developing myocardium that extended anterior and dorsal to the developing heart tube at E8.25 (Figure 6B), similar to expression of the AHF markers, *Fgf8* and *Fgf10* (Figures 3A and 6B). At E9.0, transgene expression was observed in the RV and OFT in the same domain as *Mef2c* and *Fgf10* (Figures 6C and 6D) and in the right sinus venosus (RSV) where *Mef2c* is also strongly expressed. Analysis of sections derived from these embryos further revealed transgene expression in a population of pharyngeal and splanchnic mesoderm cells that corresponds to the prospective AHF, as well as in the myocardial layer of the RV, OFT, and RSV (Figure 6D). For this transgenic line, we also observed ectopic staining in the vasculature. In contrast, there was no detectable staining in tetraploids derived from ES cells harboring the Foxh1 mutant element (Figure 6C). We also examined tetraploid embryos derived from our second Fi3A-WT ES line (S1-6), which also displayed staining in beating foci. Although overall staining was weaker in tetraploid embryos derived from this line, similar staining in the AHF and its derivatives was observed (data not shown). These results point to a key role for Foxh1 in specifying the AHF during cardiac morphogenesis in part by synergistically interacting with Nkx2-5 to regulate a TGFβ- and Smad-responsive element in the *Mef2c* gene (Figure 7).

Discussion

Foxh1 Is Required for Formation of the AHF

Cell marking studies and the analysis of a gene trap in the mouse *Fgf10* gene have shown that the major contribution of cardiogenic cells to the arterial pole of the heart occurs from the newly described AHF (Kelly and Buckingham, 2002). The AHF arises from splanchnic mesodermal cells that lie medial to the cardiac crescent and which later extend dorsally and anteriorly to the arterial pole of the developing heart. In addition, cells from the pharyngeal mesoderm contribute via the splanchnic mesoderm to expansion of the arterial pole to give rise to the RV and OFT (Kelly and Buckingham, 2002). This population of splanchnic mesoderm makes

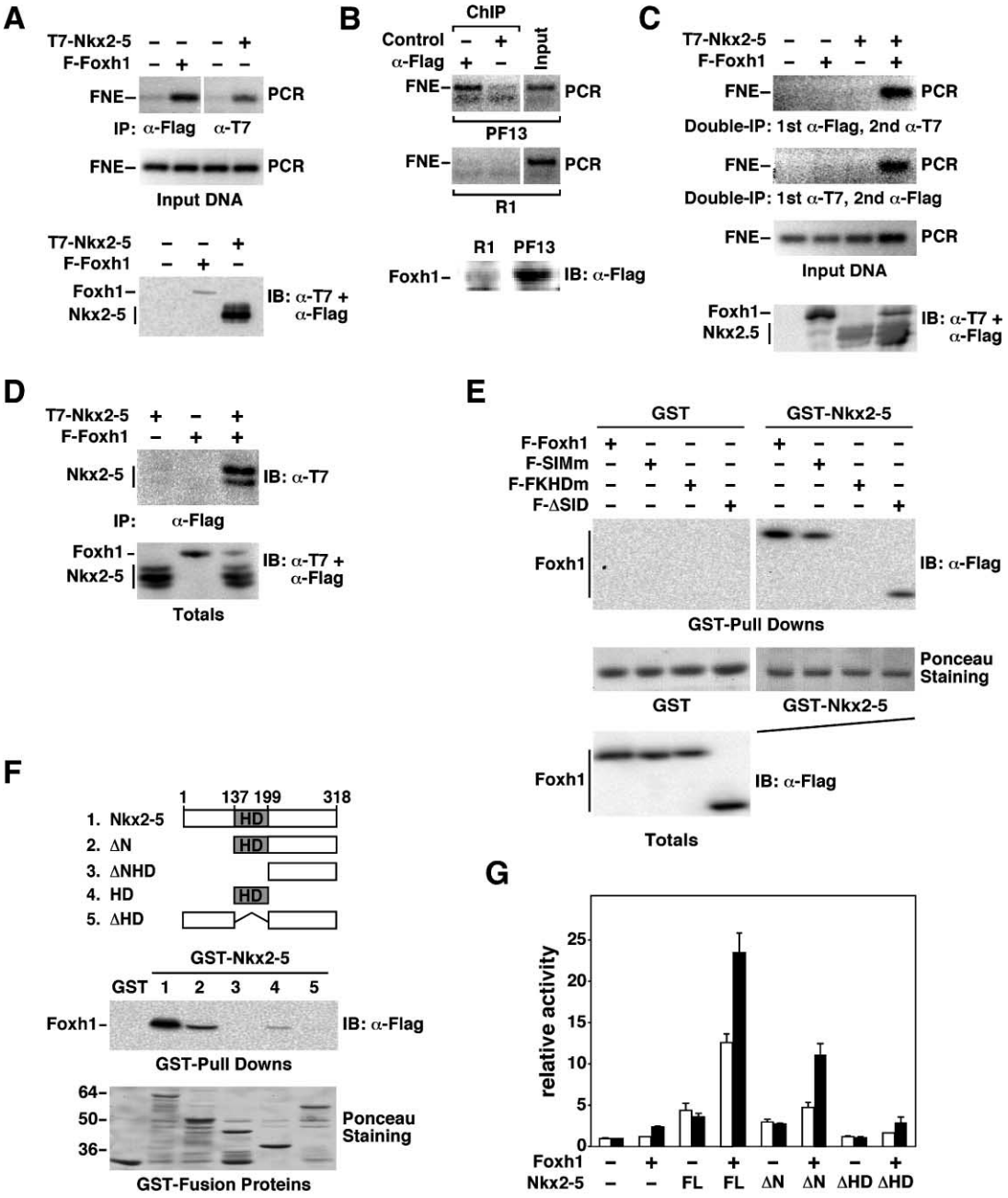

Figure 5. Physical and Functional Interactions between Foxh1 and Nkx2-5 on the FNE

(A) Both Nkx2-5 and Foxh1 occupy the FNE. COS1 cells were transfected with cDNA encoding either T7-tagged Nkx2-5 or Flag-tagged Foxh1 along with the pGL3-FNE reporter construct. Protein-DNA complexes from transfected cells were immunoprecipitated with either anti-T7 (α-T7) antibody or anti-Flag (α-Flag). Total input DNA and DNA recovered from the immunoprecipitates were analyzed by PCR. Expression of Nkx2-5 and Foxh1 was confirmed by immunoblotting (IB) using α-T7 and α-Flag monoclonal antibodies, respectively.

(B) Foxh1 occupies the endogenous FNE. Embryoid bodies obtained from *Foxh1*$^{-/-}$ ES cells reconstituted with Flag-Foxh1 (PF13) or wild-type ES cells (R1) were subjected to in vitro differentiation and a ChIP assay performed using either α-Flag antibody to immunoprecipitate Flag-Foxh1 or a control antibody. After removal of the crosslinks, immunoprecipitated DNA was amplified by PCR using *FNE*-specific primers. Expression of Flag-Foxh1 was analyzed by immunoblotting (IB) total lysates (lower panel).

(C) Foxh1 and Nkx2-5 co-occupy the FNE. COS1 cells were transfected with T7-Nkx2-5 and/or Flag-Foxh1 together with pGL3-FNE. After formaldehyde crosslinking, lysates were subjected to immunoprecipitation with the indicated antibody (1st IP), eluted with 1% SDS and then re-immunoprecipitated with α-T7 or α-Flag antibody (2nd IP). Total input FNE and FNE present in immunoprecipitates was analyzed by PCR. The expression of Nkx2-5 and Foxh1 was confirmed by immunoblotting (IB) using α-T7 and α-Flag, respectively.

(D) Nkx2-5 and Foxh1 interact. Lysates obtained from COS1 cells expressing Flag-Foxh1 and T7-Nkx2-5 either alone or together were immunoprecipitated (IP) using α-Flag antibody. Immunoprecipitates were separated by SDS-PAGE and immunoblotted (IB) using α-T7. The expression of Foxh1 and Nkx2-5 was confirmed by immunoblotting total cell lysates using α-Flag and α-T7 antibody.

(E) Foxh1 interacts with Nkx2-5 through its forkhead domain. To map the region of Foxh1 required for binding to Nkx2-5, lysates from cells expressing Flag-tagged wild-type Foxh1 (F-Foxh1), the Smad-interacting motif mutant Foxh1 (F-SIMm), the DNA binding motif mutant Foxh1

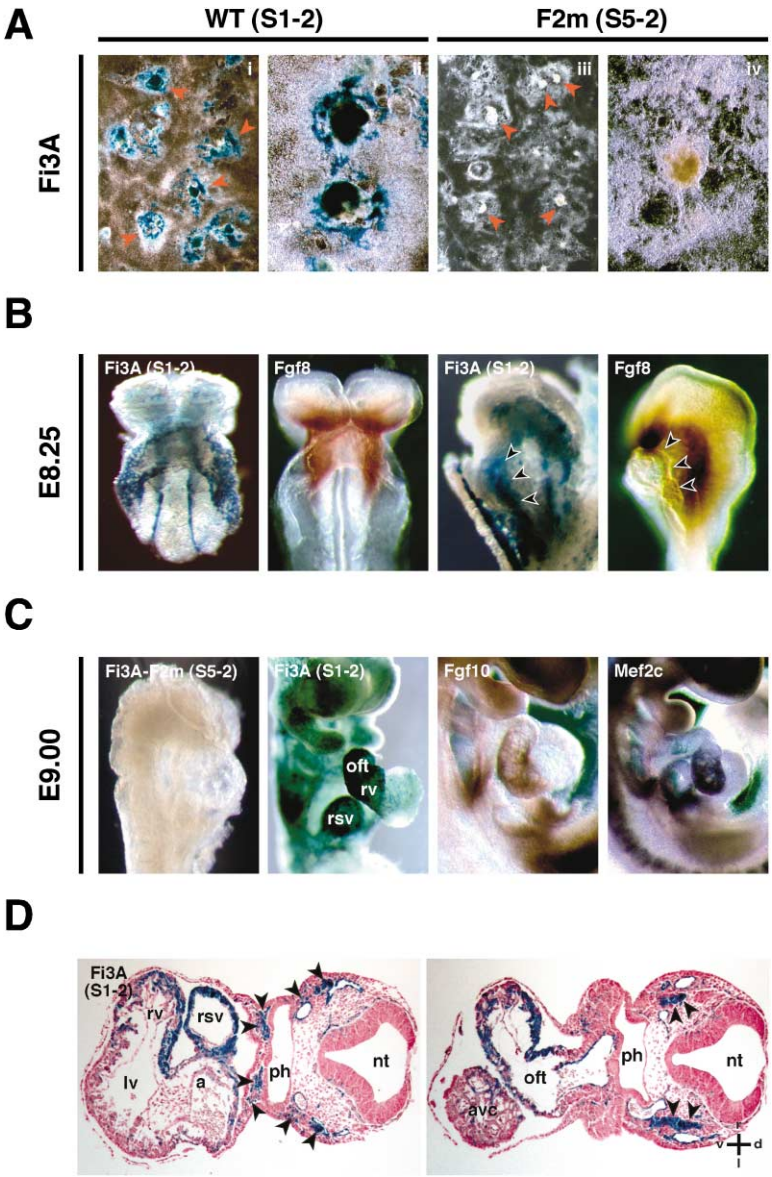

Figure 6. Expression of the *Foxh1*-Dependent *Mef2c* Intron Enhancer Fi3A

(A) Either wild-type Fi3A (WT) or Fi3A with the second Foxh1 site mutated (F2m) was coupled to hsp68LacZpA and stable transgenic ES cell lines isolated. Representative clones harboring either the WT (S1-2) or F2m mutant (S5-2) of Fi3A were subjected to in vitro differentiation and beating foci marked in each clone (red arrowheads) prior to fixation and staining for *lacZ* expression (blue).

(B and C) Analysis of *Fi3A-hsp68LacZpA* transgene expression in tetraploid embryos. Embryos derived entirely from either the S1-2 or S1-5 ES cells, harboring wild-type (Fi3A) or mutant (Fi3A-F2m) *Fi3A-hsp68LacZpA* transgene, respectively, were generated by tetraploid aggregation with B5/EGFP ICR morulae. Tetraploid embryos at E8.25 (B) or E9.0 (C) were stained for *lacZ* expression and are shown side-by-side with whole-mount in situ analysis of expression of *Fgf8* (B) or *Fgf10* and *Mef2c* (C). In the heart region, the *Fi3A-hsp68LacZpA* transgene displays an expression pattern similar to that of *Fgf8* at E8.25 and at late looping stage is strongly expressed in the RV-OFT, similar to *Fgf10* and *Mef2c*, as well as in the RSV where *Mef2c* is also expressed. Note that *Fi3A-F2m-hsp68LacZpA* (C) displays no *lacZ* expression.

(D) Transverse section of a *Fi3A-hsp68LacZpA* tetraploid embryo. At the level of the RV-LV-RSV (left panel), lacZ activity is in the myocardium of the RV and RSV, with little expression in the LV and atria, as well as in a contiguous group of pharyngeal and splanchnic mesodermal cells (arrowheads). At the level of the OFT (right panel), expression in the heart is strong throughout the OFT myocardium and in the pharyngeal mesoderm (black arrowheads).

Abbreviations: a, atrium; lv, left ventricle; oft, outflow tract; ph, pharynx; rsv, right sinus venosus; rv, right ventricle; nt, neural tube.

extensive contributions throughout the developing heart, including the atria, and is initially specified by *Isl1* (Cai et al., 2003). However, *Foxh1*$^{-/-}$ mutant hearts have severe abnormalities in OFT-RV, but have well-developed atria and a primitive left ventricle, suggesting that there are not general defects throughout the Isl1-positive splanchnic mesoderm. In support of this, *Isl1* was expressed normally in *Foxh1* mutants, as were BMPs, which are dependent on Isl1 (data not shown) (Cai et al., 2003). In contrast, *Fgf8* and *Fgf10*, which are also

(F-FKHDm), and a truncation mutant of Foxh1 that is missing the carboxy-terminal region downstream of the forkhead domain (F-ΔSID) were divided and incubated with either GST or GST-Nkx2-5 protein produced in bacteria and immobilized on glutathione-sepharose beads. After washing, Foxh1 bound to the beads was analyzed by immunoblotting (IB) using α-Flag antibody. Total GST or GST-Nkx2-5 was analyzed by staining with Ponceau S and expression of Foxh1 and its mutants confirmed by immunoblotting aliquots of total cell lysates.

(F) Nkx2-5 interacts with Foxh1 through its homeodomain. The indicated mutants of Nkx2-5 fused to GST were expressed in bacteria and purified on gluthathione sepharose beads, prior to incubating with lysates obtained from F-Foxh1-expressing cells. Foxh1 bound to the beads was analyzed by immunoblotting (IB) using α-Flag. Equivalent levels of GST-Nkx2-5 fusion proteins were confirmed by performing Ponceau S staining of the blot prior to immunoblotting. Abbreviations: HD, homeodomain; N, amino-terminal 136 amino acids.

(G) Activation of FNE by Nkx2-5 mutants. HepG2 cells were transiently transfected with the *FNE-luc* reporter construct together with the indicated Foxh1 and Nkx2-5 expression constructs. Luciferase activity in lysates from cells incubated in the absence (open bars) or presence of 200 pM TGFβ (closed bars) was determined and normalized to β-galactosidase activity, and is expressed as the mean ± SD of triplicates from a representative experiment.

expressed throughout this field in an Isl1-dependent manner, were strongly decreased but only in the anterior region. These results suggest a model in which Foxh1 functions downstream of Isl1 to specifically regulate formation of the dorsoanterior region of the AHF.

We also noted that *Foxh1*$^{-/-}$ mutants failed to pattern the outer curvature of the heart in the presumptive LV that is normally marked by expression of *Smpx* and *Nppa* (Christoffels et al., 2000). The LV expression domain of *Nppa* is dependent on Tbx5, and expression of *Tbx5* was also suppressed in the LV of mutant hearts, although not in the developing atria. Other markers of the LV and most ventricular region markers were present, suggesting that while a rudimentary LV is formed in *Foxh1*$^{-/-}$ mutants it is not fully differentiated. In contrast, we observed no significant defects in the inflow tract of *Foxh1*$^{-/-}$ mutant hearts. Thus, *Foxh1* is required for differentiation of the outer curvature of the developing LV and formation of the AHF.

Transcription Factor Networks in the AHF

Foxh1$^{-/-}$ mutant hearts have defects that closely resemble the RV and OFT defects observed in *Mef2c*$^{-/-}$ mutants (Lin et al., 1997) and *Mef2c* is not expressed in the RV-OFT of *Foxh1*$^{-/-}$ mutant hearts, although its expression in the inflow tract is retained. *Mef2c* is directly regulated by Foxh1, which physically and functionally cooperates with Nkx2-5 to mediate a strong TGFβ-dependent signal on a specific element in the *Mef2c* gene we termed the FNE. Furthermore, an intronic fragment of *Mef2c* containing the FNE drives transgene expression in the AHF and its derivatives, the RV and OFT, where *Mef2c* is strongly expressed. Regulation of Mef2c is likely to be complex, involving both initiator and maintenance elements. Thus, the FNE may not be the only element required for accurate regional expression. Indeed, expression in skeletal muscles utilizes distinct elements that control initiation and maintenance of *Mef2c* via myogenic bHLH factors (Wang et al., 2001). However, the FNE is likely a key element for Foxh1-dependent regulation of *Mef2c* in the RV and OFT derivatives of the AHF. This is consistent with recent speculation that defects in the hearts of *Mef2c*$^{-/-}$ mutants may reflect abnormalities in deployment of the AHF (Kelly and Buckingham, 2002). *Mef2c* is unlikely to be the sole target of Foxh1 in the AHF, and multiple target genes are probably involved. *Pitx2* for example, is a known target of Foxh1 and is also regulated by Nkx2-5. *Pitx2* is expressed within the branchial arch and splanchnic mesoderm that form the secondary or anterior heart field and has been shown to function there to control patterning of the OFT (Liu et al., 2002). The defects in *Pitx2* mutants are less severe than the *Foxh1* and *Mef2c* mutants and thus would be obscured in our mutant hearts. Nevertheless, these data suggest that Foxh1 regulates a broad transcriptional program that includes *Mef2c* and *Pitx2* and that these targets fulfill distinct functional roles in the AHF during heart morphogenesis.

Foxh1 has previously been suggested to be sufficient on its own to mediate strong induction of a number of target elements both in vitro and in vivo (Attisano et al., 2001), so at the molecular level it is unclear why the TGFβ-response element in the *Mef2c* gene is poorly regulated by Foxh1 alone. Nevertheless, we propose that the requirement for Nkx2-5 confers heart-specific regulation on Foxh1 targets. Interestingly, mutation of the Foxh1 or Nkx2-5 binding element or mutation of the DNA binding activity of Foxh1 or Nkx2-5 severely compromised activity on the *Mef2c* TGFβ-response element in vitro. Furthermore, analysis of an N-terminal truncation mutant of Nkx2-5, which reduces the physical interaction between Foxh1 and Nkx2-5, but not Nkx2-5 DNA binding, caused a concomitant decrease in synergistic activation. Thus Foxh1 and Nkx2-5 need to physically interact with each other and DNA in order to fully activate the TGFβ response element in the *Mef2c* gene. Physical interactions between forkhead domain proteins and homeodomain proteins were recently reported for Foxa2 with Otx2, Engrailed, Lim1, Gsc, and Hoxa5 (Foucher et al., 2003; Nakano et al., 2000) as well as between Foxd3 and Oct-4 (Guo et al., 2002). These studies showed that Foxa2 antagonized Otx2- and Engrailed-mediated activation of gene transcription (Foucher et al., 2003; Nakano et al., 2000) and that Oct4 negatively regulated Foxd3-dependent transcription (Guo et al., 2002). This contrasts the synergistic activation of Nkx2-5 and Foxh1 noted in our studies. Thus, physical interactions between forkhead and homeodomain proteins can both positively and negatively regulate downstream target genes.

Combinatorial interactions between transcription factors are a common theme in heart development (Brand, 2003; Cripps and Olson, 2002). In particular, Nkx2-5 can directly interact with Tbx5, Tbx2, Tbx20, Gata4, and Hand2 to regulate cardiac genes, in particular *Nppa*, which has an Nkx2-5-Tbx5 response element in its promoter (Bruneau et al., 2001; Brand, 2003; Cripps and Olson, 2002; Stennard et al., 2003; Thattaliyath et al., 2002). Consistent with these observations, in both *Hand2* and *Tbx5* mutant embryos, *Nppa* expression in the ventricles is disrupted. Since *Nkx2-5* expression was normal in *Foxh1*$^{-/-}$ mutants, the absence of *Nppa* expression in the mutant hearts likely reflects the loss of *Tbx5* and *Hand2* expression in the LV and RV, respectively (Figure 7). Consistent with this, we did not observe significant loss of *Actc1* expression, which can be regulated by Nkx2-5 and Gata factors. We also observed that *Smpx*, which displays an expression pattern similar to that of *Nppa*, was dependent on Foxh1. Thus, it will be of interest to see whether *Smpx* is also regulated by combinatorial interactions between Hand2, Tbx5, and Nkx2-5.

Signals Regulating Foxh1 in the AHF

Little is known of the regulatory signals that control induction and specification of the AHF. However, Foxh1 functions as a specific Smad2-Smad3 nuclear target (Labbe et al., 1998) making the Foxh1-Nkx2-5 composite *FNE* in the *Mef2c* gene dependent on an extracellular TGFβ-like signal. Accordingly, mutation of the Smad2/3 binding site on Foxh1 prevented activation of the Foxh1-Nkx2-5 response element, and when we analyzed *Foxh1*$^{-/-}$ ES cells reconstituted with the Smad binding site mutant of Foxh1, there was minimal rescue of beating foci in EB assays (I.v.B. and J.L.W., unpublished data). There are several candidate TGFβ-like factors that show temporal and spatial overlap in expression with

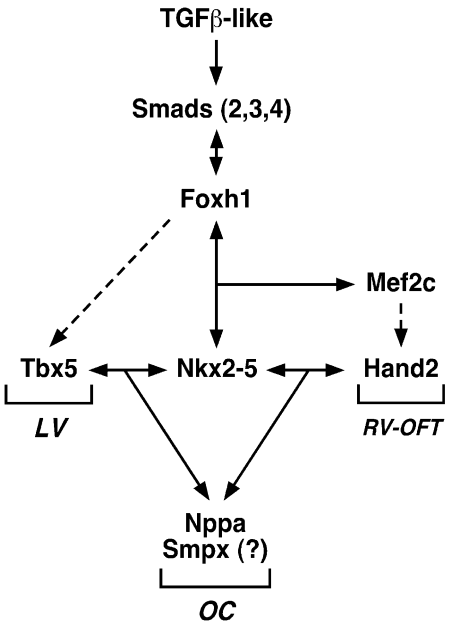

Figure 7. A Model for Foxh1 Function in the Transcriptional Regulation of Heart Development

Schematic of the role of Foxh1 in regulating the transcriptional program in the anterior heart field. Dotted lines indicate genetic interactions, whereas solid lines show direct molecular interactions.
Abbreviations: LV, left ventricle; OC, outer curvature; RV-OFT, right ventricle-outflow tract.

the stage at which the *Foxh1* heart phenotype is manifested. In particular, Nodal may contribute some of this signal (Whitman, 2001). Consistent with this, mutations in *Cfc1*, which encodes the nodal coreceptor Cripto, display heart defects (Xu et al., 1999), and in *Cfc1* null ES cells formation of beating cardiac foci is suppressed (Xu et al., 1998) similar to our findings with *Foxh1*$^{-/-}$ mutants. TGFβ itself may also play a role since *TGFβ2* is strongly expressed in the endocardium and the myocardium of the atrioventricular canal and OFT as early as E9.5, where the endocardial cushions develop (Molin et al., 2003). TGFβ would thus contribute Smad2/3-dependent signals in the anterior developing heart that might sustain Smad signaling to Foxh1 during later stages of RV and OFT development. *Nkx2-5* is expressed throughout the developing heart, yet is a key regulator of region-specific gene expression. The finding that its activity is controlled by extracellular cues that signal to binding partners such as Foxh1 thus provides a key mechanism whereby Nkx2-5-dependent gene expression can be manifested to pattern the developing heart. It will be interesting to see whether other DNA binding partners of Nkx2-5 might also be regulated by extracellular cues that control patterning in the developing heart.

schmalspur Mutants and the Zebrafish Heart

Our studies have shown a key role for Foxh1 and TGFβ signals in specifying the AHF, which forms the right side of the heart and OFT and is thus essential for pulmonary circulation. In this regard, it is notable that in zebrafish, mutations in *schmalspur*, which encodes the *Foxh1* ortholog, do not lead to heart defects, despite having defects in the gastrula organizer and formation of axial midline structures (Whitman, 2001) that are analogous to the midline defects found in the *Foxh1*$^{-/-}$ mutant mouse (Hoodless et al., 2001; Yamamoto et al., 2001). Thus it is tempting to speculate that the absence of heart defects in *Foxh1* mutant zebrafish reflects the absence of an AHF in fish, which have a single ventricle heart and no right-sided circulation. *Foxh1* may have been co-opted during evolution to mediate formation of the AHF, which is needed for elaboration of the right-sided, pulmonary circulation.

Experimental Procedures

Whole Mount RNA In Situ Hybridization, Real-Time PCR Analysis, and OPT

RNA in situ hybridizations of whole embryos were performed according to www.hhmi.ucla.edu/derobertis/ and digitally imaged on a Coolsnap. Murine probes were generous gifts, or, in the case of Foxh1, GATA6, Isl1, or Mef2c were generated in-house based on previously published work. For analysis of Mef2b and Mef2c mRNA levels, quantitative PCR was employed as described (Rebbapragada et al., 2003) using oligo p(dT)$_{20}$ primed RNA and intron-spanning primers as follows: Mef2b, forward 5′-AAGGTCCTGGAGA GAAGCTGCT-3′, reverse 5′-TCTGAAACCGACATTGCAGG-3′, which detect all Mef2b transcripts and Mef2c 'ex2..4', forward 5′-CATT GAAAACTGTGAAGTAACCTCTGG-3′, reverse 5′-CAAATCCCTGCA TTCGTTCC-3′, which detect only heart-specific Mef2c transcripts. For OPT, embryos were subjected to fluorescent whole mount in situ using a mixture of digoxigenin-labeled Mybpc3 and Actc and Rhodamine tyramide amplification (Perkin-Elmer). Embryos were imaged using an OPT device as described (Sharpe et al., 2002), data visualized using Amira software (V.3.0, TGS Inc.), and segmentation performed automatically or, when necessary, manually.

Cloning, Transcription, and Biochemical Assays

Mouse *Mef2c* enhancer fragments were PCR amplified from R1 ES cell genomic DNA and subcloned into a modified (Labbe et al., 1998) pGL3-promotor vector (Promega). The first nucleotide and length of the enhancer fragments isolated from introns (i) 3, 7, and 9 of the mouse *Mef2c* gene (Wang et al., 2001) are: Fi3A +20902 (906 bp), Fi3B +64784 (1935 bp), Fi7 +126815 (1198 bp), and Fi9 +135563 (1149 bp). Mutant versions of Foxh1 used in these studies were TGTGTATT→TTTATATT and Nkx2-5 GCAAGTG→GGAATTC. Luciferase assays in HepG2 cells were performed as described previously (Labbe et al., 1998).

Standard PCR was used to generate Foxh1 R61H;K64N forkhead mutant (FKHDm) (Pogoda et al., 2000; Sirotkin et al., 2000), Foxh1 Smad binding mutant, P371A;P372A (SIMm) (Germain et al., 2000), Foxh1 ΔSID (amino acids 1–257 of Foxh1), as well as GST- and T7-tagged Nkx2-5 and its mutant derivatives, Nkx2-5 ΔN (amino acids 137–318), Nkx2-5 ΔNHD (amino acids 200–318), Nkx2-5 HD (amino acids 137–199), and Nkx2-5 ΔHD (deletion of amino acids 137–199). Foxh1 and Nkx2-5 protein-protein interactions were performed in transiently transfected COS1 cells or using bacterially expressed proteins as previously described (Labbe et al., 1998). DNA and chromatin immunoprecipitation (ChIP) experiments were carried out as previously described (Benchabane and Wrana, 2003) using Flag-Foxh1, T7-Nkx2-5, and the FNE-luc reporter for the DNA immunoprecipitations. For endogenous ChIP, two 12-well plates of day 12 in vitro differentiated Flag-Foxh1-expressing ES cells (clone PF13) and R1 wild-type ES cells were used.

ES Cell Culture and In Vitro Differentiation Assays

The Foxh1$^{-/-}$ knock-out cell line #3 (FKO3) was previously described (Hoodless et al., 2001). Foxh1-rescued FKO3 cell lines were generated by electroporating the episomal expression vector pCAGIP containing Flag-tagged Foxh1 and expression of Flag-Foxh1 protein

in individual clones confirmed by immunoblotting. For in vitro differentiation, ES cell (Boheler et al., 2002) cultures were passaged twice on gelatin-coated plates in DMEM+ (Nagy et al., 2003), then grown to about 70% confluence. Cells were then suspended using 25 units per ml cold dispase (BD Biosciences Discovery Labware), diluted into EB medium (DMEM+ w/o LIF), and distributed into a 24-well ultra-low-attachment plate (COSTAR). Medium was changed during the next 2 days, and 5 days later EBs were transferred at low density onto gelatin-coated 12-well tissue culture plates. The number of attached EBs in each well were counted at day 7 and beating foci counted 14 days after initiation of in vitro differentiation.

To generate *Fi3A-hsp68LacZpA* transgenic ES cells, the *Mef2c* intron fragment Fi3A and the Foxh1 binding site mutant Fi3A-F2m were subcloned into pKS-hsp68LacZpA modified to contain a *puromycin* resistance cassette. Clones generated by stable transfection into R1 ES cells by electroporation were screened for *LacZ* activity after 11 days of in vitro differentiation (www.mshri.on.ca/rossant/protocols.html) and intact *Fi3A-hsp68LacZpA* transgene integration confirmed by PCR. Two clones harboring the wild-type (S1-2, S1-6) or mutant Fi3A (S5-2, S5-6) transgenes were subjected to further characterization by tetraploid-aggregation chimera analysis (Nagy et al., 2003).

Acknowledgments

The authors thank Michael Klüppel, Christine Le Roy, and Melanie Pye for advice and Benoit G. Bruneau for critical evaluation of the manuscript. We would like to thank the Transgenic Mouse Facility at Mount Sinai Hospital and Kendraprasad Harpal for advice and excellent technical assistance during this work, as well as Douglas Holmyard at the Advanced Bioimaging Centre at Mount Sinai Hospital for Scanning Electron Microscopy. For plasmids and cDNA probes we thank Rosa S. Beddington (BMP7), Benoit G. Bruneau (Nppa), Margaret Buckingham (Actc1), Kenneth R. Chien (Myl2), Sylvia Evans (Wnt11), Manfred Gessler (Hey2), Brigit L.M. Hogan (BMP2, Fgf10), Peter W. Laird (pPGKPuro), Gary E. Lyons (Myh6), Gail R. Martin (Fgf8), Eric N. Olson (Hand1), Virginia E. Papaioannou (Tbx5), Christine E. Seidman (Mybpc3), Austin Smith (pCAGIP), Deepak Srivastava (Hand2), and David B. Wilson (Gata4). This work was supported by grants to J.R., L.A., and J.L.W. from the Canadian Institutes of Health Research (CIHR) and to L.A. from the National Cancer Institute of Canada, with funds from the Canadian Cancer Society. I.v.B. was supported by the Koeln Fortune Program, Faculty of Medicine, University of Cologne and C.S. by a CIHR doctoral studentship. J.R. is a CIHR Distinguished Investigator, L.A. and J.L.W. are CIHR Investigators, and J.L.W. is an International Scholar of the Howard Hughes Medical Institute.

Received: July 8, 2004
Accepted: July 8, 2004
Published: September 13, 2004

References

Attisano, L., Silvestri, C., Izzi, L., and Labbe, E. (2001). The transcriptional role of Smads and FAST (FoxH1) in TGFβ and activin signalling. Mol. Cell. Endocrinol. *180*, 3–11.

Benchabane, H., and Wrana, J.L. (2003). GATA- and Smad1-dependent enhancers in the Smad7 gene differentially interpret bone morphogenetic protein concentrations. Mol. Cell. Biol. *23*, 6646–6661.

Boheler, K.R., Czyz, J., Tweedie, D., Yang, H.T., Anisimov, S.V., and Wobus, A.M. (2002). Differentiation of pluripotent embryonic stem cells into cardiomyocytes. Circ. Res. *91*, 189–201.

Brand, T. (2003). Heart development: molecular insights into cardiac specification and early morphogenesis. Dev. Biol. *258*, 1–19.

Bruneau, B.G., Nemer, G., Schmitt, J.P., Charron, F., Robitaille, L., Caron, S., Conner, D.A., Gessler, M., Nemer, M., Seidman, C.E., and Seidman, J.G. (2001). A murine model of Holt-Oram syndrome defines roles of the T-box transcription factor Tbx5 in cardiogenesis and disease. Cell *106*, 709–721.

Cai, C.L., Liang, X., Shi, Y., Chu, P.H., Pfaff, S.L., Chen, J., and Evans, S. (2003). Isl1 identifies a cardiac progenitor population that proliferates prior to differentiation and contributes a majority of cells to the heart. Dev. Cell *5*, 877–889.

Christoffels, V.M., Habets, P.E., Franco, D., Campione, M., de Jong, F., Lamers, W.H., Bao, Z.Z., Palmer, S., Biben, C., Harvey, R.P., and Moorman, A.F. (2000). Chamber formation and morphogenesis in the developing mammalian heart. Dev. Biol. *223*, 266–278.

Cripps, R.M., and Olson, E.N. (2002). Control of cardiac development by an evolutionarily conserved transcriptional network. Dev. Biol. *246*, 14–28.

Dufort, D., Schwartz, L., Harpal, K., and Rossant, J. (1998). The transcription factor HNF3beta is required in visceral endoderm for normal primitive streak morphogenesis. Development *125*, 3015–3025.

Foucher, I., Montesinos, M.L., Volovitch, M., Prochiantz, A., and Trembleau, A. (2003). Joint regulation of the MAP1B promoter by HNF3beta/Foxa2 and Engrailed is the result of a highly conserved mechanism for direct interaction of homeoproteins and Fox transcription factors. Development *130*, 1867–1876.

Germain, S., Howell, M., Esslemont, G.M., and Hill, C.S. (2000). Homeodomain and winged-helix transcription factors recruit activated Smads to distinct promoter elements via a common Smad interaction motif. Genes Dev. *14*, 435–451.

Guo, Y., Costa, R., Ramsey, H., Starnes, T., Vance, G., Robertson, K., Kelley, M., Reinbold, R., Scholer, H., and Hromas, R. (2002). The embryonic stem cell transcription factors Oct-4 and FoxD3 interact to regulate endodermal-specific promoter expression. Proc. Natl. Acad. Sci. USA *99*, 3663–3667.

Harvey, R.P. (2002a). Molecular determinants of cardiac development and congenital disease. In Mouse Development: Patterning, Morphogenesis, and Organogenesis., J. Rossant and P.P.L. Tam, eds. (San Diego: Academic Press), pp. 331–370.

Harvey, R.P. (2002b). Patterning the vertebrate heart. Nat. Rev. Genet. *3*, 544–556.

Hoodless, P.A., Pye, M., Chazaud, C., Labbe, E., Attisano, L., Rossant, J., and Wrana, J.L. (2001). FoxH1 (Fast) functions to specify the anterior primitive streak in the mouse. Genes Dev. *15*, 1257–1271.

Kelly, R.G., and Buckingham, M.E. (2002). The anterior heart-forming field: voyage to the arterial pole of the heart. Trends Genet. *18*, 210–216.

Kelly, R.G., Brown, N.A., and Buckingham, M.E. (2001). The arterial pole of the mouse heart forms from Fgf10-expressing cells in pharyngeal mesoderm. Dev. Cell *1*, 435–440.

Labbe, E., Silvestri, C., Hoodless, P.A., Wrana, J.L., and Attisano, L. (1998). Smad2 and Smad3 positively and negatively regulate TGFβ-dependent transcription through the forkhead DNA-binding protein FAST2. Mol. Cell *2*, 109–120.

Lin, Q., Schwarz, J., Bucana, C., and Olson, E.N. (1997). Control of mouse cardiac morphogenesis and myogenesis by transcription factor MEF2C. Science *276*, 1404–1407.

Liu, C., Liu, W., Palie, J., Lu, M.F., Brown, N.A., and Martin, J.F. (2002). Pitx2c patterns anterior myocardium and aortic arch vessels and is required for local cell movement into atrioventricular cushions. Development *129*, 5081–5091.

Mjaatvedt, C.H., Nakaoka, T., Moreno-Rodriguez, R., Norris, R.A., Kern, M.J., Eisenberg, C.A., Turner, D., and Markwald, R.R. (2001). The outflow tract of the heart is recruited from a novel heart-forming field. Dev. Biol. *238*, 97–109.

Molin, D.G., Bartram, U., Van der Heiden, K., Van Iperen, L., Speer, C.P., Hierck, B.P., Poelmann, R.E., and Gittenberger-de-Groot, A.C. (2003). Expression patterns of Tgfbeta1–3 associate with myocardialisation of the outflow tract and the development of the epicardium and the fibrous heart skeleton. Dev. Dyn. *227*, 431–444.

Nagy, A., Gertsenstein, M., Vintersten, K., and Behringer, R. (2003). Manipulating the Mouse Embryo: A Laboratory Manual, 3rd edn (New York: CSHL Press).

Nakano, T., Murata, T., Matsuo, I., and Aizawa, S. (2000). OTX2 directly interacts with LIM1 and HNF-3beta. Biochem. Biophys. Res. Commun. *267*, 64–70.

Olson, E.N., and Schneider, M.D. (2003). Sizing up the heart: development redux in disease. Genes Dev. *17*, 1937–1956.

Parmacek, M.S., and Leiden, J.M. (1999). GATA transcription factors and cardiac development. In Heart Development, R.P. Harvey and N. Rosenthal, eds. (San Diego: Academic Press), pp. 291–306.

Pogoda, H.M., Solnica-Krezel, L., Driever, W., and Meyer, D. (2000). The zebrafish forkhead transcription factor FoxH1/Fast1 is a modulator of nodal signaling required for organizer formation. Curr. Biol. *10*, 1041–1049.

Rebbapragada, A., Benchabane, H., Wrana, J.L., Celeste, A.J., and Attisano, L. (2003). Myostatin signals through a transforming growth factor beta-like signaling pathway to block adipogenesis. Mol. Cell. Biol. *23*, 7230–7242.

Schwartz, R.J., and Olson, E.N. (1999). Building the heart piece by piece: modularity of cis-elements regulating Nkx2–5 transcription. Development *126*, 4187–4192.

Sharpe, J., Ahlgren, U., Perry, P., Hill, B., Ross, A., Hecksher-Sorensen, J., Baldock, R., and Davidson, D. (2002). Optical projection tomography as a tool for 3D microscopy and gene expression studies. Science *296*, 541–545.

Sirotkin, H.I., Gates, M.A., Kelly, P.D., Schier, A.F., and Talbot, W.S. (2000). Fast1 is required for the development of dorsal axial structures in zebrafish. Curr. Biol. *10*, 1051–1054.

Srivastava, D., Thomas, T., Lin, Q., Kirby, M.L., Brown, D., and Olson, E.N. (1997). Regulation of cardiac mesodermal and neural crest development by the bHLH transcription factor, dHAND. Nat. Genet. *16*, 154–160.

Stennard, F.A., Costa, M.W., Elliott, D.A., Rankin, S., Haast, S.J., Lai, D., McDonald, L.P., Niederreither, K., Dolle, P., Bruneau, B.G., et al. (2003). Cardiac T-box factor Tbx20 directly interacts with Nkx2–5, GATA4, and GATA5 in regulation of gene expression in the developing heart. Dev. Biol. *262*, 206–224.

Thattaliyath, B.D., Firulli, B.A., and Firulli, A.B. (2002). The basic-helix-loop-helix transcription factor HAND2 directly regulates transcription of the atrial naturetic peptide gene. J. Mol. Cell. Cardiol. *34*, 1335–1344.

Thomas, T., Yamagishi, H., Overbeek, P.A., Olson, E.N., and Srivastava, D. (1998). The bHLH factors, dHAND and eHAND, specify pulmonary and systemic cardiac ventricles independent of left-right sidedness. Dev. Biol. *196*, 228–236.

Waldo, K.L., Kumiski, D.H., Wallis, K.T., Stadt, H.A., Hutson, M.R., Platt, D.H., and Kirby, M.L. (2001). Conotruncal myocardium arises from a secondary heart field. Development *128*, 3179–3188.

Wang, D.Z., Valdez, M.R., McAnally, J., Richardson, J., and Olson, E.N. (2001). The Mef2c gene is a direct transcriptional target of myogenic bHLH and MEF2 proteins during skeletal muscle development. Development *128*, 4623–4633.

Weisberg, E., Winnier, G.E., Chen, X., Farnsworth, C.L., Hogan, B.L., and Whitman, M. (1998). A mouse homologue of FAST-1 transduces TGF beta superfamily signals and is expressed during early embryogenesis. Mech. Dev. *79*, 17–27.

Whitman, M. (2001). Nodal signaling in early vertebrate embryos: themes and variations. Dev. Cell *1*, 605–617.

Xu, C., Liguori, G., Adamson, E.D., and Persico, M.G. (1998). Specific arrest of cardiogenesis in cultured embryonic stem cells lacking Cripto-1. Dev. Biol. *196*, 237–247.

Xu, C., Liguori, G., Persico, M.G., and Adamson, E.D. (1999). Abrogation of the Cripto gene in mouse leads to failure of postgastrulation morphogenesis and lack of differentiation of cardiomyocytes. Development *126*, 483–494.

Yamamoto, M., Meno, C., Sakai, Y., Shiratori, H., Mochida, K., Ikawa, Y., Saijoh, Y., and Hamada, H. (2001). The transcription factor FoxH1 (FAST) mediates Nodal signaling during anterior-posterior patterning and node formation in the mouse. Genes Dev. *15*, 1242–1256.